Polymer 49 (2008) 4576–4584

Contents lists available at ScienceDirect

Polymer

journal homepage: www.elsevier.com/locate/polymer

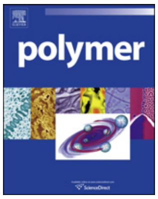

Synthesis and characterization of polypropylene-based polymer hybrids linking poly(methyl methacrylate) and poly(2-hydroxyethyl methacrylate)

Hideyuki Kaneko*, Junji Saito, Nobuo Kawahara, Shingo Matsuo, Tomoaki Matsugi, Norio Kashiwa

Research Center, Mitsui Chemicals, Inc., 580-32 Nagaura, Sodegaura, Chiba 299-0265, Japan

ARTICLE INFO

Article history:
Received 26 May 2008
Received in revised form 11 August 2008
Accepted 13 August 2008
Available online 23 August 2008

Keywords:
Polypropylene
Radical polymerization
Graft copolymer

ABSTRACT

Isotactic polypropylene-based polymer hybrids linking poly(methyl methacrylate) (PMMA) and poly(2-hydroxyethyl methacrylate) (PHEMA) were successfully synthesized by a graft copolymerization from maleic anhydride-modified polypropylene (PP-MAH). PP-MAH reacted with ethanolamine to produce a hydroxyl group containing polypropylene (PP-OH) and the thus obtained PP-OH was treated with 2-bromoisobutyryl bromide and converted to a 2-bromoisobutyryl group containing polypropylene (PP-Br). The metal-catalyzed radical polymerization of MMA with PP-Br was performed using a copper catalyst system in *o*-xylene solution at 100 °C to give the PP-based polymer hybrids linking PMMA segments (PP–PMMA hybrids). Thus obtained PP–PMMA hybrids demonstrated higher melting temperature than PP-Br and microphase-separation morphology at the nanometer level owing to the chemical linkage between both segments. On the other hand, the polymer hybrids linking PHEMA segment (PP–PHEMA hybrids) were also obtained by the radical polymerization of HEMA with PP-Br in *o*-xylene slurry at 25 °C. TEM observation suggested that the polymerization mainly initiated on the surface of the PP-Br powder, led to the peculiar core–shell-like morphology. These PP–PHEMA hybrid powders showed a good affinity with water due to the hydrophilicity of the PHEMA segments.

1. Introduction

Recent advances in polyolefin (PO) chemistry have led to the creation of PO-based polymer hybrids between PO segments and other PO or polar polymer segments, which were prepared by several post-polymerization processes, such as radical [1–10], anionic [11–14], cationic [15,16] and coordination polymerizations [17–19], or a polymer coupling reaction using functionalized POs [20–23]. In particular, combinations of POs and polar polymers by chemical linkage have been attracting a lot of attention as PO hybrids between different segments such as crystalline/amorphous, polar/nonpolar or hydrophilic/hydrophobic segments. They are expected to bring some improved and unique properties to the ordinary POs to broaden the applications of POs into highly profitable fields, including compatibilizer, impact modifier, adhesion, coating, ionomer, antistatic agent, biocompatible material, stimulus-sensitive material and so on. For example, it is well known that the introduction of polar segments into PO backbone often enables them to be used as compatibilizer or modifier in polymer blends and composites.

Some of these PO hybrids can be produced by a post-polymerization process with PO macroinitiators, which are obtained by transforming a variety of functionalized POs to radical or anionic polymerization initiators. To prepare the functionalized POs, several kinds of methods using chain transfer reaction at olefin polymerization, olefin copolymerization with polar monomers and chemical modification of terminally unsaturated POs have been reported. For example, Chung et al. reported the syntheses of block and graft copolymers by using borane- and *p*-methylstyrene-containing POs, which were obtained by chain transfer reaction or copolymerization, in combination with radical, anionic and ring-opening anionic polymerization of various polar monomers such as methyl methacrylate (MMA), styrene (St) and ε-caprolactone [1,11,12,24]. In our previous work, we reported on the functionalized polyethylene (PE) with reactive groups such as hydroxyl [25] or amino [26] groups under precise control of the positions of the functional groups. In particular, this methodology can selectively prepare both the terminally functionalized PE and the functionalized branch-grafted PE. Their reactive groups can be easily converted to initiation sites for the various polymerization systems, such as transition-metal-catalyzed radical polymerization, reversible addition–fragmentation chain transfer (RAFT) polymerization and ring-opening anionic polymerization. The combination of these site-selective functionalized POs and various polymerization

---

* Corresponding author. Tel.: +81 438 64 2319; fax: +81 438 64 2370.
E-mail address: hideyuki.kaneko@mitsui-chem.co.jp (H. Kaneko).

0032-3861/$ – see front matter © 2008 Elsevier Ltd. All rights reserved.
doi:10.1016/j.polymer.2008.08.032

processes gave a variety of block and graft copolymers such as PE-*b*-PMMA block copolymers [2,3], PE-*g*-PMMA and PE-*g*-poly(*n*-butyl acrylate) graft copolymers [4], PE-*g*-poly(propylene glycol) and PE-*g*-poly(ε-caprolactone) graft copolymers [13]. In addition, there are some examples of the PO-based graft copolymers produced by radical or anionic polymerization with functionalized POs [5,6,14]. These functionalization methods of POs, however, need unusual olefin polymerization conditions in the presence of specific chain transfer agents or polar monomers, which are poisonous for most olefin polymerization catalysts to retard the polymerization. Therefore, the type of POs and the polymerization conditions are generally restricted.

Alternatively, it has been well known that some commercially available functionalized POs are produced by a direct copolymerization or a radical grafting method. Many types of ethylene copolymers with polar monomers, such as vinyl acetate, ethyl acrylate, glycidyl methacrylate and so on, are produced by direct radical copolymerization under a high pressure process. Chemical modification is one of the useful approaches to prepare the PO macroinitiators. For example, Matyjaszewski et al. reported that PE macroinitiators prepared from commercially available poly(ethylene-*co*-glycidyl methacrylate) initiated atom transfer radical polymerization of St and MMA, leading to the corresponding PE-*g*-polystyrene and PE-*g*-PMMA [7].

On the other hand, the radical grafting of polar monomers on POs is also an important method for preparing functionalized POs and the incorporation of many kinds of polar monomers, such as methacrylates, acrylates, styrene and so on, has been reported [8,9]. Maleic anhydride-modified PO (PO-MAH) is well known as a commercially available functionalized PO and many types of PO-MAH with various MAH contents, molecular weights and olefin compositions have been industrially produced. Compared with the direct copolymerization method, this method has the advantage in that it can provide not only ethylenic but also propylenic and higher α-olefinic polymers. Because of its accessibility and high reactivity, PO-MAHs are widely used for various purposes such as additives, adhesives, coatings and compatibilizers for polymer blends. Furthermore, they can be also used as a building block for the PO-based graft copolymers. For example, coupling reactions of them with the other polymer chains possessing some reactive functional groups give the corresponding graft copolymers, such as PO–PO [20], PO–polyamide [21], PO–polyester [22] and PO–polyurethane [23]. However, there are few reports on graft copolymers syntheses via the graft copolymerization using macroinitiators derived from PO-MAHs [10].

In this article, we herein introduce the PP-based polymer hybrids linking PMMA or poly(2-hydroxyethyl methacrylate) (PHEMA) using a new synthetic method through a combination of PP-MAH and metal-catalyzed radical polymerization. In addition, we also discuss their unique characteristics and properties demonstrated by thermal analysis and transmission electron microscopy (TEM) observation.

2. Experimental

2.1. General procedures and materials

All manipulations of air- and water-sensitive materials were preformed under a dry nitrogen atmosphere in a conventional nitrogen-filled glove box. CuBr, *N*,*N*,*N*′,*N*″,*N*″-pentamethyldiethylenetriamine (PMDETA), ethanolamine, triethylamine and 2-bromoisobutyryl bromide (BiBB) were purchased from Wako Pure Chemical Industries and used without further purification. MMA and HEMA (Wako Pure Chemical Industries) were dried over CaH_2 and distilled *in vacuo*. *o*-Xylene used as a solvent was dried over Al_2O_3 and degassed by bubbling with N_2 gas. Maleic anhydride-modified polypropylene (PP-MAH) was prepared in the conventional way [27]. From GPC measurement and ^1H NMR analysis, the number average molecular weight of the obtained PP-MAH was 33,000 and the content of MAH was 0.14 mol% as shown in Table 1.

Table 1
Summary of functionalization of PP

Sample	Content of functional group	M_w[c]	M_n[c]	M_w/M_n[c]	Functionality[d] unit/chain
PP-MAH	MAH, 0.14 mol%[a]	95,700	33,000	2.9	1.1
PP-OH	OH, 0.13 mol%[a]	139,000	36,900	3.8	1.2
PP-Br	Br, 0.25 wt%[b]	114,000	33,600	3.4	1.1

[a] Determined by ^1H NMR.
[b] Determined by ion chromatography.
[c] Measured at 140 °C in 1,2-dichlorobenzene with PP calibration.
[d] Calculated from the content of functional group and M_n.

2.2. Preparation of PP macroinitiator (PP-Br)

A typical process is as follows: *o*-xylene (700 mL) and PP-MAH (75 g, 2.5 mmol-MAH) were placed in a 1-L glass reactor equipped with a mechanical stir bar and then PP-MAH was dissolved at 120 °C for 3 h under a nitrogen atmosphere. Then, ethanolamine (200 mL, 3.3 mmol) was added and the mixture was maintained at 120 °C for 6 h under stirring. The reaction mixture was poured into 2 L of acetone. The precipitated polymer was collected by filtration, washed with acetone and dried *in vacuo* at 80 °C for 10 h to give 75.1 g of hydroxyl group containing PP (PP-OH) as a white powder. Thus obtained PP-OH (71 g) and toluene (700 mL) were placed in a 1-L glass reactor equipped with a mechanical stir bar and then PP-OH was dissolved at 105 °C for 2 h under a nitrogen atmosphere. Triethylamine (8.1 mL, 54.4 mmol) and BiBB (6.7 mL, 54.4 mmol) were added to the reactor and the mixture was stirred at 105 °C for 2 h. The reaction mixture was poured into 2 L of methanol. The resulting polymer was collected by filtration, washed with methanol and dried *in vacuo* at 80 °C for 10 h to give 71 g of 2-bromoisobutyryl group containing PP (PP-Br).

2.3. MMA polymerization with PP macroinitiator

A typical polymerization process (for Run 4 in Table 1) is as follows: PP-Br (15 g, 0.47 mmol as 2-bromoisobutyryl group) and *o*-xylene (100 mL) were placed in a 500-mL glass reactor equipped with a mechanical stir bar and then PP-Br was dissolved at 100 °C for 2 h under nitrogen atmosphere. Then, MMA (3.8 mL) and a solution of CuBr/PMDETA in *o*-xylene (0.89 mmol as a copper atom and 1.78 mmol as PMDETA, pretreated for 5 min at ambient temperature) were added to the reactor and the mixture was maintained at 100 °C for 4 h under stirring. After adding 200 mL of toluene and cooling, the reaction mixture was poured into 1.5 L of methanol and the white solid was collected by filtration, washed with methanol and dried *in vacuo* at 80 °C for 10 h. As shown in Table 2, three kinds of polymers were obtained.

2.4. HEMA polymerization with PP macroinitiator

A typical polymerization process (for Run 4 in Table 3) is as follows: PP-Br (15 g, 0.47 mmol as 2-bromoisobutyryl group) and *o*-xylene (250 mL) were placed in a 500-mL glass reactor equipped with a mechanical stir bar and PP-Br was dissolved at 130 °C for 1 h under nitrogen atmosphere. Then the obtained solution was cooled to 25 °C for 2 h under stirring to give the slurry of the precipitated PP-Br in *o*-xylene. HEMA (4.3 mL) and a solution of CuBr/PMDETA in *o*-xylene (0.89 mmol as a copper atom and 1.78 mmol as PMDETA, pretreated for 5 min at ambient temperature) were added to the reactor and the mixture was maintained at 25 °C for 4 h

Table 2
Summary of MMA polymerization[a]

Sample	PP-Br (g)[d]	MMA (mL)	CuBr (mmol)	Yield (g)	THF Insoluble part[e] (wt%)	MMA content[f]	
						(mol%)	(wt%)
PP–PMMA1	15.0	3.8	0.89	16.0	98.4	2.9	6.6
PP–PMMA2	15.0	9.5	0.89	18.3	97.6	8.4	17.9
PP–PMMA3	15.0	53.2	0.89	30.0	96.7	25.9	45.5
PP–PMMA4[b]	3.0	10.6	0.18	2.9	–	n.d.	n.d.
PP–PMMA5[c]	3.0	10.6	0	3.1	93.0	n.d.	n.d.

[a] Polymerization conditions: $[\text{PP-Br}]_0/[\text{CuBr}]_0/[\text{PMDETA}]_0 = 1/1.9/3.8$ (molar ratio) in 100 mL of *o*-xylene at 100 °C for 4 h.
[b] PP-OH was used in place of PP-Br. Polymerization conditions: $[\text{CuBr}]_0/[\text{PMDETA}]_0 = 1/2$ (molar ratio) in 20 mL of *o*-xylene at 100 °C for 4 h.
[c] Polymerization conditions: $[\text{PP-Br}]_0/[\text{CuBr}]_0/[\text{PMDETA}]_0 = 1/0/0$ (molar ratio) in 20 mL of *o*-xylene at 100 °C for 4 h.
[d] 0.031 mmol of Br/g of polymer.
[e] Determined by Soxhlet extraction in boiling THF for 9 h.
[f] Determined by ^{1}H NMR for THF insoluble part. n.d. = not determined.

Table 3
GPC data of PP-Br before and after MMA polymerization[a]

Sample	M_w	M_n	M_w/M_n
PP-Br	168,000	48,600	3.4
PP–PMMA1	416,000	42,400	9.8
PP–PMMA2	671,000	47,700	14.1
PP–PMMA3	714,000	49,000	14.6

[a] Measured at 140 °C in 1,2-dichlorobenzene with PS calibration.

under stirring. Then, the resulting slurry was poured into 1.5 L of methanol and the white solid was collected by filtration, washed with methanol and dried *in vacuo* at 80 °C for 10 h. As shown in Table 5, two kinds of polymers were obtained.

2.5. Preparation of the blended polymers

A typical procedure is as follows: the polymers (*ca.* 1 g as a total amount) and *o*-xylene (30 mL) were added to a 100-mL glass reactor equipped with a magnetic stir bar and were stirred at 130 °C until the polymer mixture was homogeneous (*ca.* 2 h). The blended polymer was precipitated into cold methanol (400 mL) and then dried *in vacuo* at 80 °C for 10 h.

2.6. Analytical procedures

^{1}H NMR spectra were recorded on JEOL GSX-400 (400 MHz) spectrometers using 1,2-dichlorobenzene-d_4 as a solvent at 120 °C. The gel permeation chromatograms (GPC) calibrated with PP were recorded by using a Waters Alliance GPC2000 equipped with four TSKgel columns (two sets of TSKgelGMH6-HT and two sets of TSKgelGMH6-HTL) and a refractive index detector at 140 °C in 1,2-dichlorobenzene and those calibrated with PS standard were recorded by using a CFC T-150A (Mitsubishi Kagaku Corp.) equipped with three columns (Shodex AT-806MS) and an IR spectrometer Miran 1ACVF at 140 °C in 1,2-dichlorobenzene. Elemental analysis for CHN was carried out on a Perkin–Elmer 2400II type analyzer and that for O was carried out on an Elementar vario EL III type analyzer. Attenuated total reflection infrared (ATR/IR) spectra were recorded on a Varian FTS-6000 FT-IR spectrometer over a spectral range from 4000 to 400 cm^{-1} at a resolution of 2 cm^{-1} (32 cumulative scans). A thin film for IR analysis was prepared by a compression molding at 250 °C. For the determination of bromine content in PP-Br, PP-Br was pretreated by oxygen flask combustion method and analyzed using a Dionex DX-500 ion chromatography system consisting of two columns (IonPac AS12A and IonPac AG12A) and a suppressed conductivity detector. The peak melting temperature of the polymers was measured by using Seiko Instruments RDC220 differential scanning calorimeter. The DSC curves were recorded during the second heating cycle from 30 to 200 °C, with a heating rate of 10 °C/min.

2.7. Transmission electron microscopy (TEM) observations

Ultrathin (*ca.* 100 nm) sections of the polymer, which had been pressed into a sheet, were cut on a Reica Ultracut microtome equipped with a diamond knife at a low temperature and were then stained with RuO$_4$. TEM observations were made with a Hitachi H-7000 transmission electron microscope at an acceleration voltage of 75 kV and at a magnification of 5000, 20,000 and 100,000.

3. Results and discussion

3.1. Synthesis of PP macroinitiators

The synthetic route of PP macroinitiators is shown in Scheme 1. In the first step, the succinic anhydride (SA) group grafted in PP-MAH reacted with excess ethanolamine to give the PP with *N*-(2-hydroxyethyl)succinimide group (PP-OH). The reaction was performed in *o*-xylene solution at 120 °C. In the second step, PP-OH reacted with 2-bromoisobutyryl bromide to produce PP-Br, which has 2-bromoisobutyryl groups as an initiation site for the metal-catalyzed radical polymerization. In general, the bromination reaction is preferably performed under mild conditions to avoid any side reactions. However, in the case of crystalline polyolefins such as polyethylene and polypropylene, high temperature and long holding time are often needed to complete the reaction owing to low solubility and low hydroxyl group concentration [2,4,28]. Therefore, in this case the reaction was carried out in toluene solution at 105 °C through the addition of an excess amount of 2-bromoisobutyryl bromide and triethylamine. Fig. 1 shows the IR spectra of PP-Br and its precursors, PP-MAH and PP-OH. In Fig. 1(a), the absorption bands for C=O stretching vibration of SA group were observed around 1800 cm^{-1}. After a reaction with ethanolamine, the absorption bands for C=O stretching vibration at 1770 and 1700 cm^{-1} appeared as shown in Fig. 1(b). These absorption bands would be able to be assigned to a succinimide group, suggesting that SA group predominantly reacted with amino group rather than hydroxyl group of ethanolamine. In Fig. 1(c), new absorption bands for C=O stretching vibration of an ester group at 1740 cm^{-1} were observed in addition to the

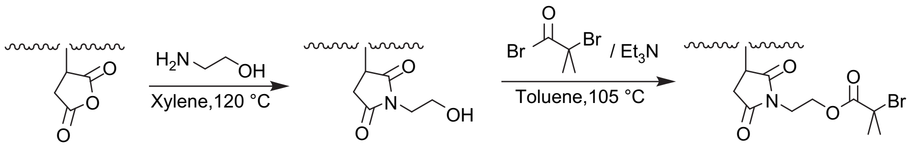

PP-MAH **PP-OH** **PP-Br**

Scheme 1. Synthesis of PP-Br.

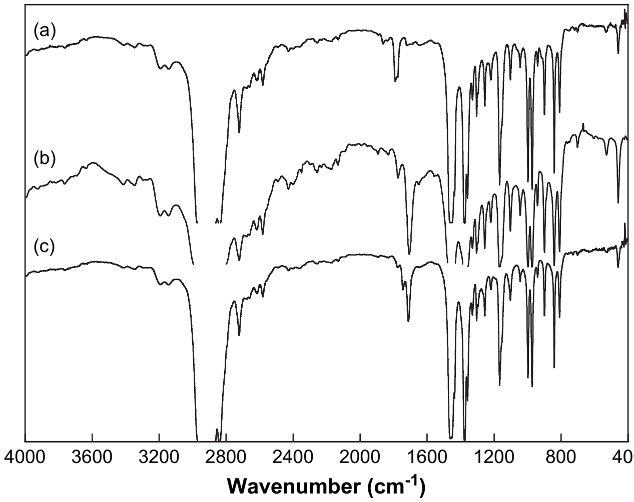

Fig. 1. IR spectra of (a) PP-MAH, (b) PP-OH and (c) PP-Br.

succinimide group. These results of IR analysis obviously indicate a successful progress of the expected functionalization reactions as shown in Scheme 1.

Fig. 2 shows ^1H NMR spectra of PP-Br and its precursors, PP-MAH and PP-OH. For PP-MAH (Fig. 2(a)), the broad and multiple signals of δ 2.5–3.25 ppm would be assigned to the protons of the SA ring ($-CH_2-CH\langle$) and the signals of the PP backbone were observed at δ 0.7–2.0 ppm. For PP-OH (Fig. 2(b)), two broad signals of δ 3.60 and 3.65 ppm correspond to two kinds of methylene protons ($\rangle N-CH_2-CH_2-OH$) and the signals of the SA ring observed in (a) slightly shifted to the higher magnetic field (δ 2.4–3.05 ppm), which would show that the SA group was converted to the succinimide group by the reaction with ethanolamine. The relative intensities of the signals at 3.65, 3.60 and 2.4–3.05 ppm were roughly estimated to be 2/2/3, respectively, indicating the existence of the *N*-(2-hydroxyethyl) succinimide group. For PP-Br (Fig. 2(c)), in addition to the signals of the succinimide ring, the signals of methylene protons ($\rangle N-CH_2-CH_2-OCO-$) and methyl protons ($-OCOC(CH_3)_2Br$) were observed at 4.25, 3.70 and 1.85 ppm, respectively. Because the resolution of ^1H NMR spectrum for PP-Br was not enough to determine the content of 2-bromoisobutyrate group, a bromine content in PP-Br was analyzed by ion chromatography and estimated to be 0.25 wt%. Assuming all of the detected bromine atoms attribute to 2-bromoisobutyrate group, its content can be calculated to be 0.13 mol%, indicating that more than 90% of SA groups in the starting PP-MAH were converted into the 2-bromoisobutyrate group. These functionalization results are summarized in Table 1. It can be seen that molecular weight and molecular weight distribution of PP-OH and PP-Br were higher than those of PP-MAH. One of the reasons for these results might be because the coupling reaction between PP-OH and PP-MAH occurred to give the higher molecular weight component. However, both samples completely dissolve in toluene at 110 °C and therefore, such portion would be vanishingly small. From the number average molecular weight of the obtained PP-Br, the average number of the 2-bromoisobutyrate group in PP-Br can be estimated to be 1.1 units per chain. Namely, all of the PP backbones averagely have one initiation site. The thus obtained PP-Br was used as a macroinitiator for the metal-catalyzed radical polymerization.

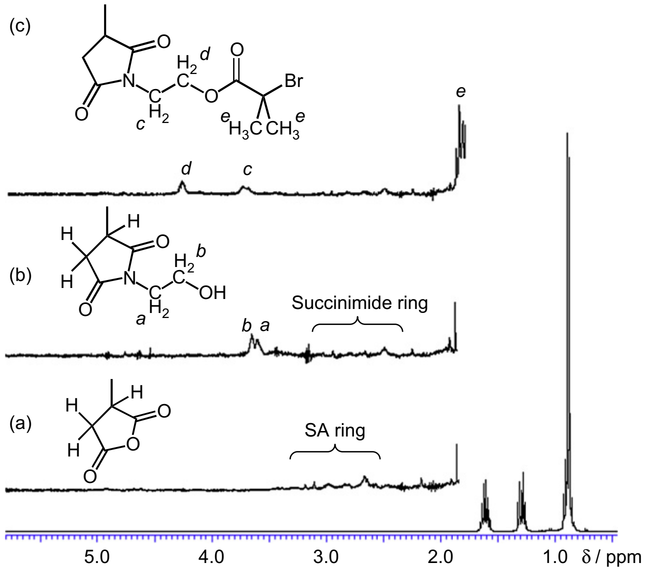

Fig. 2. ^1H NMR spectra of (a) PP-MAH, (b) PP-OH and (c) PP-Br (400 MHz in 1,2-dichlorobenzene-d_4 at 120 °C).

3.2. Radical polymerization of MMA initiated by PP macroinitiator

It is well known that the metal-catalyzed radical polymerization enabled controlled polymerization of various vinyl monomers, represented by (meth)acrylates and styrenes, to give the precisely controlled polymers [29,30]. In particular, it is an effective method for the syntheses of block and graft copolymers using macroinitiators. We applied this method to create the polymer hybrids linking between PO and polar polymers. The polymerization of MMA with a PP macroinitiator was carried out in an *o*-xylene solution using CuBr/PMDETA as a catalyst system. Table 2 summarizes the results by altering polymerization conditions. Because of high molecular weight of PP macroinitiator, a significant amount of *o*-xylene was needed to dissolve the PP macroinitiator and reduce the viscosity in the early stage of polymerization, resulting in very low concentration of initiation sites in this polymerization system. Therefore, the excess amount of catalyst had to be used for achieving sufficient initiation and propagation rate as shown in Table 2. In the case of PP–PMMA1, 2 and 3, the viscosity of the polymerization system increased as polymerization time increased and this suggested the progress of MMA polymerization to give a polymer with higher molecular weight compared with the starting PP macroinitiator. The polymerization was stopped by cooling the reactor with an ice bath. The resulting mixture was poured into methanol and the precipitated polymer was collected by filtration. To remove the homo-PMMA produced by thermal polymerization, the obtained polymers were purified by the Soxhlet extraction with boiling THF. In each sample, the extracted fraction was only a small amount, suggesting that most of the consumed monomer was grafted onto the PP backbone. In contrast, when PP-OH was used as a macroinitiator in place of PP-Br (PP–PMMA4), the polymer yield did not increase. In addition, the graft polymerization did not proceed in the absence of catalyst (PP–PMMA5).

The obtained copolymers purified by Soxhlet extraction were analyzed at 120 °C by ^1H NMR in 1,2-dichlorobenzene-d_4 as a solvent. Fig. 3 shows the ^1H NMR spectra of the purified copolymers. From the integrated intensities of the signals at δ 3.52 ppm (methyl ester protons of the PMMA segment) and δ 0.8–2.3 ppm (propylene unit and PMMA backbone), each copolymer contained 6.6, 17.9 and 45.5 wt% of PMMA segment, respectively. Furthermore, the signals of methylene protons adjacent to the ester group ($-CH_2-OCO-$) were shifted to the slightly higher magnetic field in comparison with the PP-Br as shown in Fig. 4. This indicates that

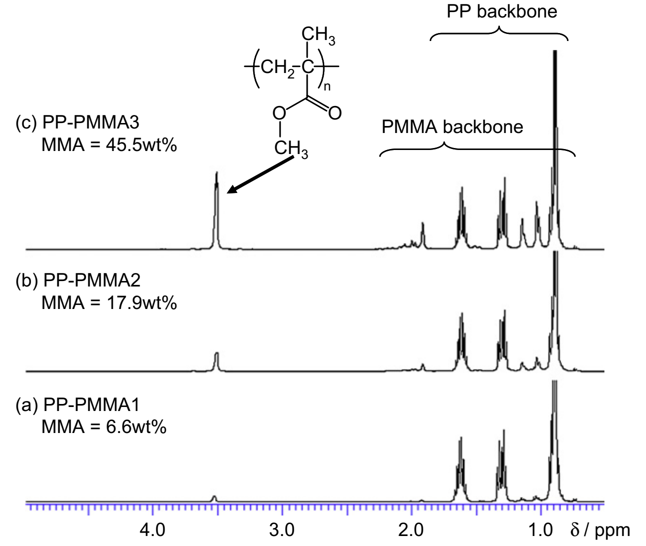

Fig. 3. ^{1}H NMR spectra of the polymer hybrids. (a) PP–PMMA1, (b) PP–PMMA2 and (c) PP–PMMA3 (400 MHz, in 1,2-dichlorobenzene-d_4 at 120 °C).

the polymerization would be initiated at the 2-bromoisobutyryl group in the PP-Br and its initiation efficiency may be nearly complete [31]. The GPC traces of PP-Br and purified polymers are shown in Fig. 5. Since GPC curves were maintained monomodal molecular weight distribution after MMA polymerization, the obtained polymers had almost no PMMA homopolymers with extremely high molecular weight, which might be generated by thermal polymerization at 100 °C. The top peak of the GPC curve gradually shifted to higher molecular weight region as the MMA content increased, which indicated the successful graft copolymerization onto the PP-Br macroinitiator. The data derived from GPC measurement are shown in Table 3. The weight average molecular weight of PP–PMMA copolymers obviously increased with increasing MMA content. However, the number average molecular weight of PP–PMMA1 and PP–PMMA2 was lower than that of PP-Br and the molecular weight distribution of PP–PMMA copolymer was significantly broadened. Although these phenomena would suggest the poorly controlled polymerization of MMA owing to high polymerization temperature, at least it was confirmed that the PP-based polymer hybrids linking PMMA segment (PP–PMMA hybrid) were obtained by MMA polymerization with PP-Br and the resulting polymers mainly consist of the PP-*g*-PMMA graft copolymer.

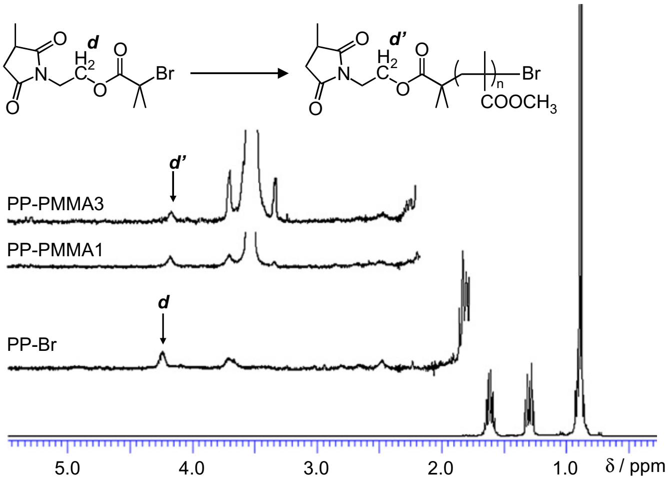

Fig. 4. Evolution of the ^{1}H NMR signals of the initiating species during the polymerization of MMA with PP-Br (400 MHz, in 1,2-dichlorobenzene-d_4 at 120 °C).

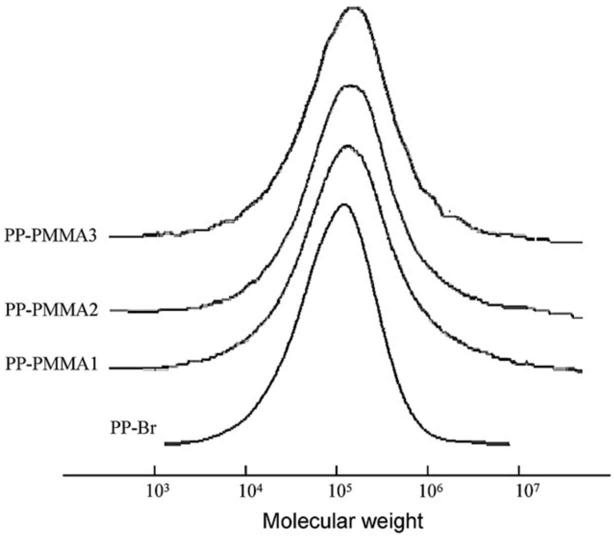

Fig. 5. GPC traces of PP-Br before and after MMA polymerization.

Table 4 summarizes the DSC results of PP macroinitiator and the obtained PP–PMMA hybrids. The thermogram of each sample was recorded in the second heating run at 10 °C/min to eliminate the thermal history. In all samples, it is clear that the peak melting temperatures (T_ms) at around 160 °C show the PP segments in the backbone and heat of fusion (ΔH) gradually decreased with increasing MMA content of the hybrid. The relative crystallinity, which is calculated by the ΔH of the hybrid divided by the ΔH of the PP-Br and the wt% of PP in the hybrid, can be used to estimate the crystallinity of the PP part in the hybrid compared to PP-Br [11]. In spite of increase of the MMA content, the relative crystallinities of the PP part in the hybrids are nearly constant. This result suggests that PMMA segments grafted on the PP backbone would not disturb the crystallization of PP segments at least within 45.5 wt% of MMA content.

3.3. *Morphology of PP–PMMA hybrids*

The morphology of these PP–PMMA hybrids was observed by TEM, as shown in Fig. 6. Despite the different MMA contents, the microphase-separation morphology at the nanometer level between the PP phase (stained by RuO_4) and the PMMA phase (unstained by RuO_4) was observed in all samples, indicating the chemical linkage between both segments. In the cases of the low and middle MMA contents (6.6 and 17.9 wt%, Fig. 6(a) and 6(b)), both phases finely dispersed and the distinction as to which phase was matrix was impossible. On the other hand, in the case of higher

Table 4
Summary of DSC results for PP-Br and PP–PMMA hybrids

Sample	MMA content[a] (wt%)	T_m[b] (°C)	ΔH[b] (J/g)	Relative crystallinity of PP part[c] (%)
PP-Br	0	157.1	91.5	100
PP–PMMA1	6.6	160.0	83.7	98
PP–PMMA2	17.9	159.2, 146.5	75.9	101
PP–PMMA3	45.5	162.2, 148.2	54.0	108

[a] Determined by ^{1}H NMR for THF insoluble part.
[b] Observed by DSC measurement.
[c] Relative crystallinity (%) = $[\Delta H_{PP-PMMA}/(\Delta H_{PP\text{-}Br} \times \text{weight ratio of PP in the PP–PMMA hybrid})] \times 100$.

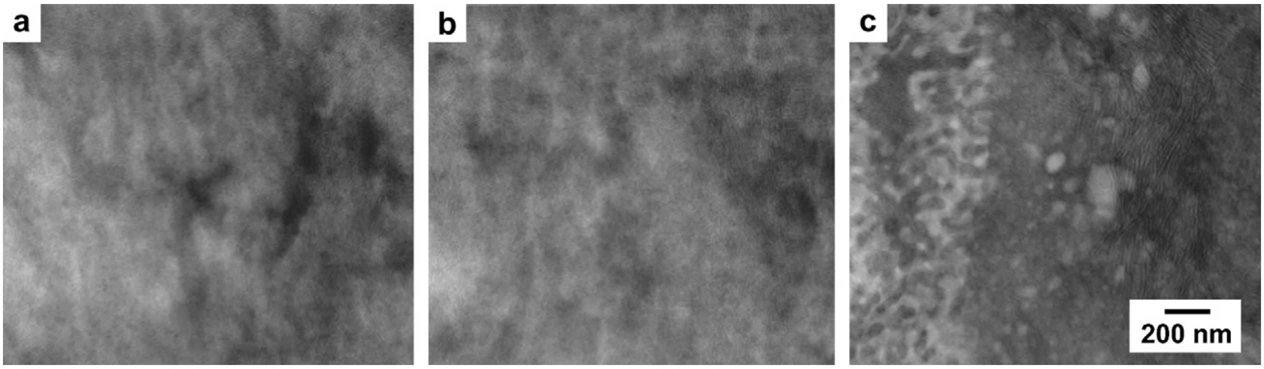

Fig. 6. TEM images of the PP–PMMA hybrids with different MMA contents. (a) 6.6, (b) 17.9 and (c) 45.5 wt%.

MMA content (45.5 wt%, (c)) the PMMA domains were partially observed. It is thought that these domains formed by the aggregation of the longer PMMA segments grafted on PP backbone.

3.4. *Compatibility of PP–PMMA hybrids for PP/PMMA blend*

Because the polymer hybrids obtained in this study consist of two segments with a different nature, such as PP and PMMA, they can be expected to work as a compatibilizer for improving the interfacial interactions between blended polymers. To evaluate this effectiveness, each PP–PMMA hybrid was added to homo-PP/homo-PMMA blended system in an *o*-xylene solution at 130 °C. For comparison, a blended sample without the hybrid was also prepared. Fig. 7 shows the TEM images of the blended polymers with the hybrid and the optical micrograph of the blended polymer without the hybrid. The blended polymers with the hybrid (Fig. 7(a) and (b)) showed a morphology in which the size of the dispersed domains was significantly smaller than that of the blended polymer without the hybrid (Fig. 7(c)). In addition, the morphologies between two kinds of blended polymers with the hybrids were almost the same. It would seem that these polymer hybrids effectively work as a compatibilizer for PP/PMMA blended polymer and the compatibility of the PP–PMMA hybrid is independent of its MMA content at least in a range of 6.6–45.5 wt%.

Fig. 8 shows the DSC thermograms of PP and PP/PMMA blended polymers without and with the PP–PMMA hybrids. In cooling thermograms as shown in Fig. 8(a), the peak crystallization temperature of the PP/PMMA blended polymer (116.5 °C) was higher than that of only PP (114.3 °C) and the addition of PP–PMMA1 and PP–PMMA3 remarkably increased the peak crystallization temperature (121.7 and 122.7 °C, respectively). In addition, the peak melting temperature as shown in Fig. 8(b) also showed the same tendency of the peak crystallization temperature and particularly, the hybrid with higher MMA content (PP–PMMA3, 45.5 wt%) was very effective for increasing the melting temperature. These phenomena show that the well-dispersed PMMA domains also worked as efficient nucleating agents for the crystallization of PP matrix like inorganic nanoparticle, clay and organic salts [32–34].

3.5. *Radical polymerization of HEMA initiated by PP macroinitiator*

2-Hydroxyethyl methacrylate (HEMA) is one of the typical methacrylate monomers possessing a functional group and it is well known that its homopolymer (PHEMA) has hydrophilicity. Therefore, the polymer hybrid combining PO with PHEMA is expected to be a new PO-based material with a hydrophilic nature. We successfully obtained the PP-based polymer hybrids linking PHEMA segments through the metal-catalyzed radical polymerization using a PP macroinitiator (PP-Br) for the first time. The polymerization of HEMA initiated by PP-Br was carried out at 25 °C in *o*-xylene with a CuBr/PMDETA catalyst system. Table 5 shows the result of HEMA polymerization. Although the PP macroinitiator did not dissolve in *o*-xylene under this condition, the polymerization of HEMA proceeded easily and most of the monomer was consumed in only 4 h. On the other hand, PP-OH did not initiate the polymerization and the polymerization without catalyst did not proceed as in the case of MMA (PP–PHEMA3 and 4). To remove the homopolymer (PHEMA) produced by the thermal polymerization, the obtained polymers were purified by the Soxhlet extraction with boiling DMF, which is a good solvent for PHEMA and a poor solvent for PP. In the case of PP–PHEMA1 and 2, the extracted fraction was less than 5 wt% of the obtained polymer, indicating that the graft polymerization of HEMA proceeded efficiently.

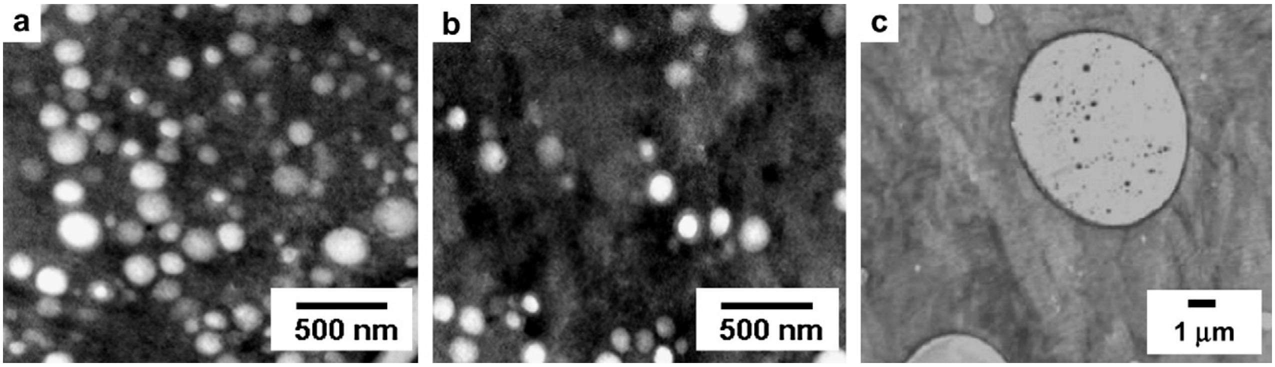

Fig. 7. TEM images of homo-PP/homo-PMMA blended polymer with the PP–PMMA hybrid with MMA contents of (a) 6.6 and (b) 45.5 wt% (PP/PMMA/PP–PMMA hybrid = 70/30/10 w/w/w) and (c) homo-PP/homo-PMMA blended polymer without the PP–PMMA hybrid (PP/PMMA = 70/30 w/w).

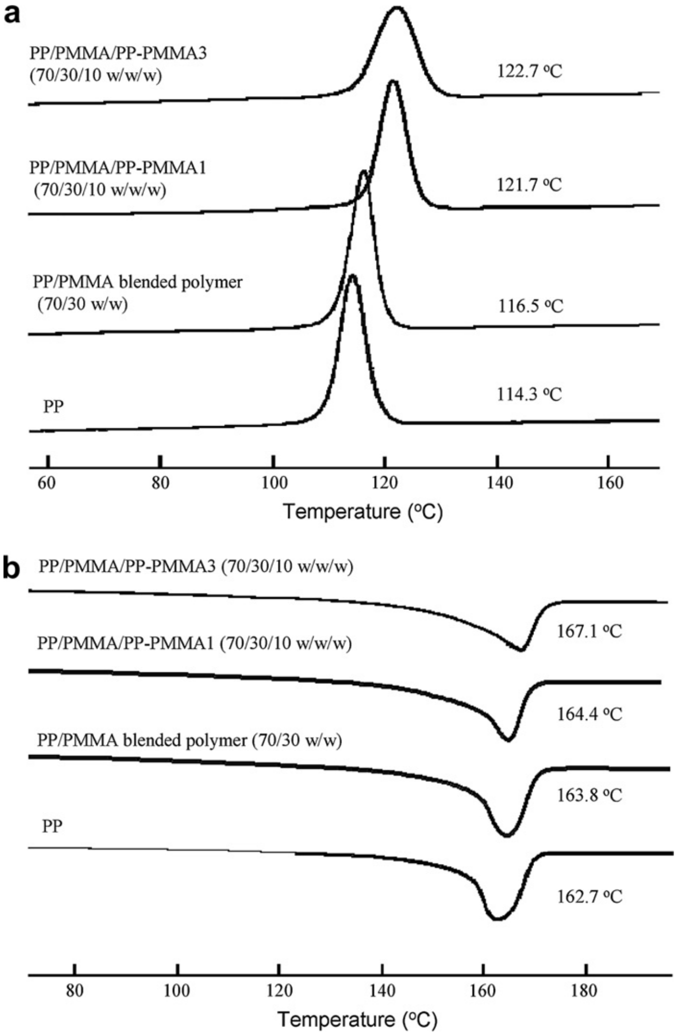

Fig. 8. DSC cooling thermograms (a) and heating thermograms (b) for PP and PP/PMMA blended polymers without and with the PP–PMMA hybrids.

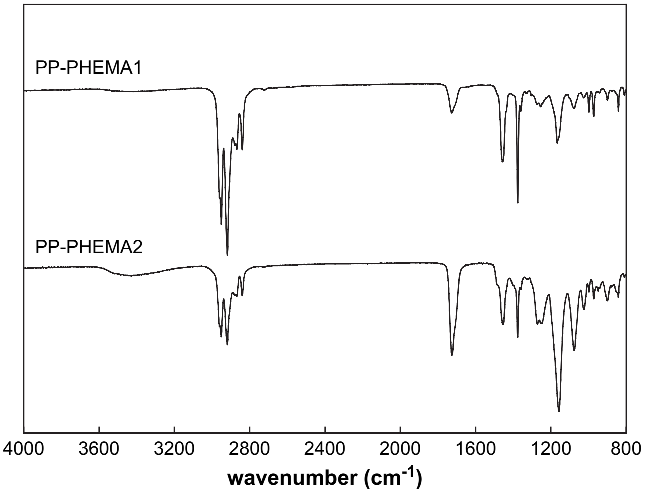

Fig. 9. ATR/IR spectra of PP–PHEMA hybrids with different HEMA contents.

Since the obtained polymers were rigid and brittle, it was so difficult to prepare the thin and transparent film for normal FT-IR analysis. Then, the existence of PHEMA segment in these polymers was confirmed by the attenuated total reflection infrared (ATR/IR) analysis of the molded press sheet as shown in Fig. 9. In these spectra, the absorption bands for C═O stretching vibration centered at 1727 cm^{-1} and O–H stretching vibration at 3600–3200 cm^{-1} show the existence of PHEMA segment and the absorption band at 3000–2800 cm^{-1} can be assigned to C–H stretching vibration of PP segment. We tried to determine the HEMA contents in these purified polymers by using ^{1}H NMR, however, selecting a good solvent for both PP and PHEMA segments was difficult so that their monomer compositions could not be determined by ^{1}H NMR. Instead, elemental analysis was used for the determination of monomer composition. As shown in Table 6, the oxygen content in these obtained polymers was higher than that in PP-Br, suggesting the introduction of PHEMA segment and the formation of the PP–PHEMA hybrid. From the contents of each element, the HEMA contents of PP–PHMEA1 and PP–PHEMA2 were estimated to be 26.5 and 60.0 wt%, respectively.

Table 7 summarizes the DSC results of the purified PP–PHEMA hybrids. As in the case with the PP–PMMA polymer hybrids, the peak melting temperature of the PP–PHEMA hybrid was higher than that of PP-Br and the heat of fusion gradually decreased with increased HEMA content. On the other hand, the relative crystallinity of the PP part did not decrease in spite of the higher HEMA content as the PP–PMMA hybrids.

3.6. *TEM observation of the PP–PHEMA hybrid powder*

Fig. 10 shows TEM micrographs of the cross-section of the PP–PHEMA hybrid powders with 26.5 and 60.0 wt% of HEMA contents. The TEM images at a magnification of 5000 times (Fig. 10(A) and (B)) reveal that the obtained powders consisted of two phases with a different brightness. Since the PHEMA segment is more easily stained by RuO_4 than the PP segment, it is considered that the interior of the particle is the PP-rich phase and the surface of the powder is the PHEMA-rich phase. From the observation at high magnification as shown in

Table 5
Summary of HEMA polymerization[a]

Sample	PP-Br[d] (g)	HEMA (mL)	CuBr (mmol)	Yield (g)	DMF insoluble part[e] (wt%)	HEMA content[f] (wt%)
PP–PHEMA1	15.0	4.3	0.89	18.8	95.4	26.5
PP–PHEMA2	15.0	16.7	0.89	31.5	96.0	60.0
PP–PHEMA3[b]	3.0	3.3	0.18	2.9	–	n.d.
PP–PHEMA4[c]	3.0	3.3	0	2.9	–	n.d.

[a] Polymerization conditions: $[\text{PP-Br}]_0/[\text{CuBr}]_0/[\text{PMDETA}]_0 = 1/1.9/3.8$ (molar ratio) in 250 mL of *o*-xylene at 25 °C for 4 h.
[b] PP-OH was used in place of PP-Br. Polymerization conditions: $[\text{CuBr}]_0/[\text{PMDETA}]_0 = 1/2$ (molar ratio) in 50 mL of *o*-xylene at 25 °C for 4 h.
[c] Polymerization conditions: $[\text{PP-Br}]_0/[\text{CuBr}]_0/[\text{PMDETA}]_0 = 1/0/0$ (molar ratio) in 50 mL of *o*-xylene at 25 °C for 4 h.
[d] 0.031 mmol of Br/g of polymer.
[e] Determined by Soxhlet extraction in boiling DMF for 12 h.
[f] Determined by elemental analysis for DMF insoluble part. n.d. = not determined.

Table 6
Elemental analysis data for PP-Br and PP–PHEMA hybrids

Sample	C/H/N/O	
	Found	Calc'd
PP-Br	84.9/14.2/<0.3/0.6	–
PP–PHEMA1	77.1/12.4/<0.3/10.2	77.1/12.5/0.2/10.2 (as HEMA cont.: 26.5 wt%)
PP–PHEMA2	67.0/10.4/<0.3/22.3	67.2/10.3/0.1/22.4 (as HEMA cont.: 60.0 wt%)

Table 7
Summary of DSC results for PP–PHEMA hybrids

Sample	HEMA content[a] (wt%)	T_{m}[b] (°C)	ΔH[b] (J/g)	Relative crystallinity of PP[c] part (%)
PP-Br	0	157.1	91.5	100
PP–PHEMA1	26.5	160.6	71.7	107
PP–PHEMA2	60.0	159.4	36.1	99

[a] Determined by elemental analysis for DMF insoluble part.

[b] Observed by DSC measurement.

[c] Relative crystallinity (%) = $[\Delta H_{\mathrm{PP–PHEMA}}/(\Delta H_{\mathrm{PP\text{-}Br}} \times$ weight ratio of PP in the PP–PHEMA hybrid$)] \times 100$.

Fig. 10(C) and (D), the thickness of the surface layer of each powder is estimated to be about 80 and 300 nm, respectively. Because these values of thickness were too small for the HEMA content, it can be suggested that the PHEMA chain grows not only on the surface of the PP powder but also under the surface of the PP powder, probably at the amorphous part, to give a peculiar core–shell-like morphology.

3.7. Hydrophilicity of the PP–PHEMA hybrids

Fig. 11 shows the behavior of PP-Br and polymer hybrids in water. In the case of PP-Br and the PP–PHEMA hybrid with lower HEMA content (Fig. 11(A) and 11(B)), the polymer powder floated on water. On the other hand, the PP–PHEMA hybrid powders with higher HEMA content (60.0 wt%, in Fig. 11(C)) were well suspended in water. These phenomena clearly demonstrate that the PHEMA segment was properly grafted on the surface of the PP powder, which led to an increase in the affinity with water because of its hydrophilicity. Alternatively, the densities of the PP and PHEMA segments were determined to be 0.91 and 1.27 g/cm^3, respectively [35]. Therefore, this distinctive behavior might be due to not only the hydrophilicity but also the density among each graft copolymer.

4. Conclusions

PP macroinitiator was prepared by the reaction between maleic anhydride-modified PP and ethanolamine and the subsequent reaction with 2-bromoisobutyryl bromide. The obtained PP macroinitiator was successfully employed for the radical polymerization of MMA and

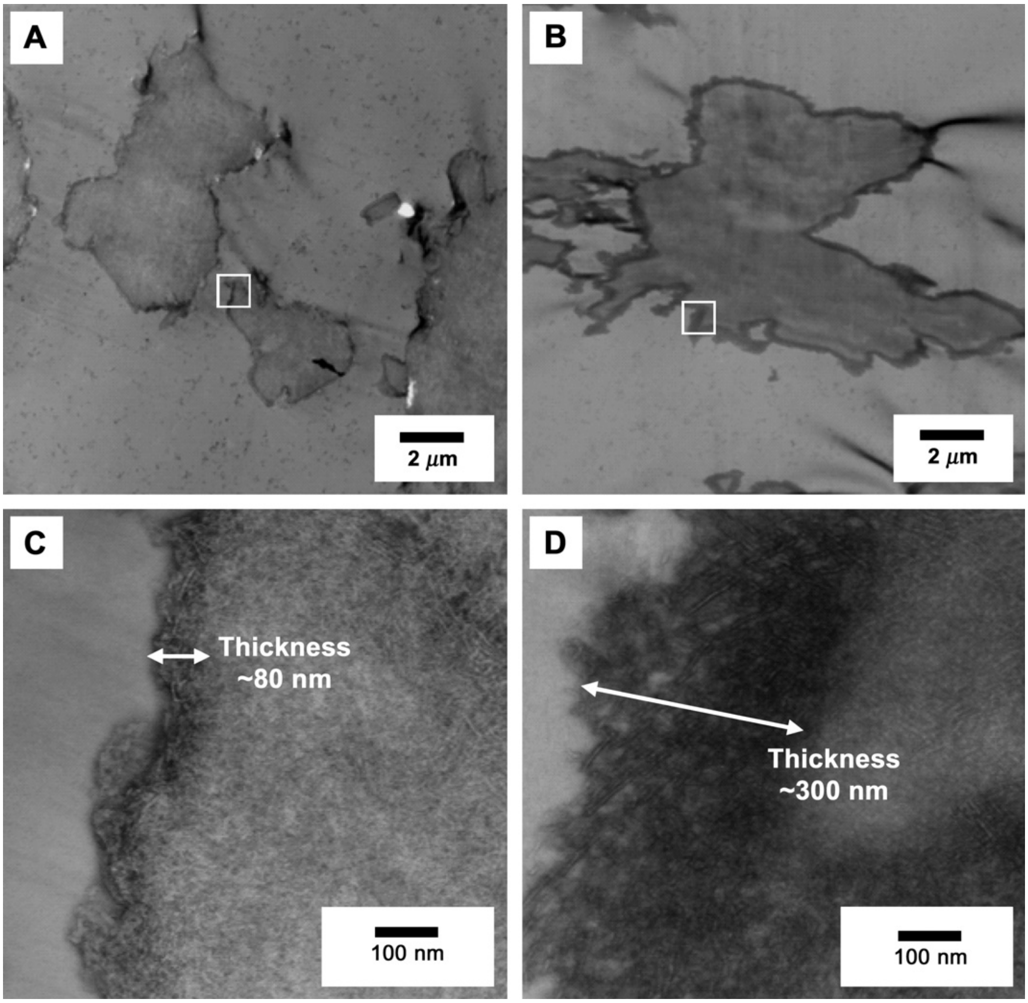

Fig. 10. TEM images of the cross-section of the PP–PHEMA hybrid powders: (A) PP–PHEMA1 and (B) PP–PHEMA2 at a magnification of 5000 times and (C) PP–PHEMA1 and (D) PP–PHEMA2 at a magnification of 100,000 times.

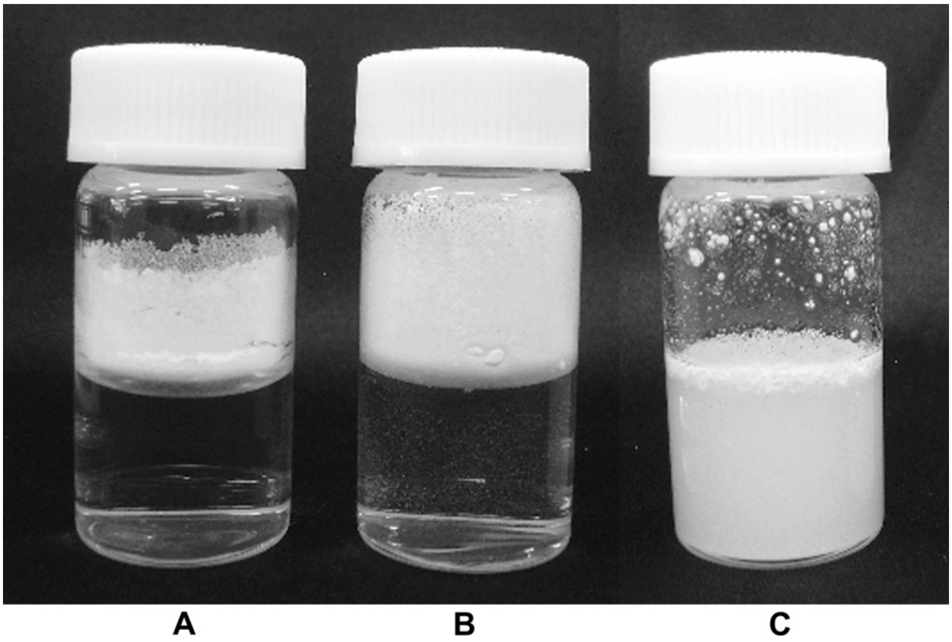

Fig. 11. Pictures of (A) PP-Br and PP–PHEMA hybrids with HEMA contents of (B) 26.5 and (C) 60.0 wt% in water.

HEMA using a CuBr/PMDETA catalyst system to give the corresponding polymer hybrids. In the case of MMA polymerization, the polymerization proceeded in a solution condition and the MMA content of the obtained polymers was confirmed to be in the range of 6.6–45.5 wt% by ^{1}H NMR analysis. From TEM observation of these polymer hybrids, the PP and PMMA segments finely dispersed at the nanometer level and these hybrids worked as a good compatibilizer for the PP/PMMA polymer blend. In the case of HEMA polymerization, the polymerization proceeded in slurry conditions resulting in the polymer hybrids with 26.5 and 60.0 wt% of HEMA contents. TEM micrographs of the cross-section of the obtained PP–PHEMA hybrid powder revealed a core–shell structure consisting of a PP-rich core and a PHEMA-rich shell. In addition, the core–shell hybrid with higher HEMA content showed an affinity for water because of the modification of the PP powder surface by the incorporation of the PHEMA segment. The introduction of PMMA and PHEMA segments into PP improved its low interfacial interaction with polar polymers or water and thus obtained PP hybrids are expected to be used as not only compatibilizer and modifier but also the other new applications such as antistatic agent, antifog additive, aqueous coating and aqueous emulsion. Thus, the polymer hybrids with chemical linkage between PP and the other polymers are useful as a new material possessing unique and improved properties reflecting the kind and content of the grafted polar segments.

References

[1] Chung TC, Rhubright D, Jiang GJ. Macromolecules 1993;26:3467–71.
[2] Matsugi T, Kojoh S, Kawahara N, Matsuo S, Kaneko H, Kashiwa N. J Polym Sci Part A Polym Chem 2003;41:3965–73.
[3] Kawahara N, Kojoh S, Matsuo S, Kaneko H, Matsugi T, Saito J, et al. Polym Bull 2006;57:805–12.
[4] Inoue Y, Matsugi T, Kashiwa N, Matyjaszewski K. Macromolecules 2004;37:3651–8.
[5] Stehling UM, Malmström EE, Waymouth RM, Hawker CJ. Macromolecules 1998;31:4396–8.
[6] Liu S, Sen A. Macromolecules 2001;34:1529–32.
[7] Matyjaszewski K, Teodorescu M, Miller PJ, Peterson ML. J Polym Sci Part A Polym Chem 2000;38:2440–8.
[8] Moad G. Prog Polym Sci 1999;24:81–142.
[9] Rätzsch M, Arnold M, Borsig E, Bucka H, Reichelt N. Prog Polym Sci 2002;27:1195–282.
[10] Steinert V, Reinhardt S, Werner K. J Polym Sci Part A Polym Chem 1999;37:2045–54.
[11] Chung TC, Rhubright D. Macromolecules 1994;27:1313–9.
[12] Chung TC, Lu HL, Ding RD. Macromolecules 1997;30:1272–8.
[13] Kashiwa N, Matsugi T, Kojoh S, Kaneko H, Kawahara N, Matsuo S, et al. J Polym Sci Part A Polym Chem 2003;41:3657–66.
[14] Caporaso L, Iudici N, Oliva L. Macromol Symp 2006;234:42–50.
[15] Kennedy JP, Vidal A. J Polym Sci Polym Chem Ed 1975;13:1765–81.
[16] Kennedy JP, Vidal A. J Polym Sci Polym Chem Ed 1975;13:2269–76.
[17] Hosoda S, Kihara H, Kojima K, Satoh Y, Doi Y. Polym J 1991;23:277–84.
[18] Yasuda H, Furo M, Yamamoto H, Nakamura A, Miyake S, Kibino N. Macromolecules 1992;25:5115–6.
[19] Desurmont G, Tokimitsu T, Yasuda H. Macromolecules 2000;33:7679–81.
[20] Kashiwa N, Kojoh S, Kawahara N, Matsuo S, Kaneko H, Matsugi T. Macromol Symp 2003;201:319–26.
[21] Li H, Chiba T, Higashida N, Yang Y, Inoue T. Polymer 1997;38:3921–5.
[22] Sun Y-J, Hu G-H, Lambla M, Kotlar HK. Polymer 1996;37:4119–27.
[23] Lu Q-W, Macosko CW. Polymer 2004;45:1981–91.
[24] Chung TC. Prog Polym Sci 2002;27:39–85.
[25] Imuta J, Kashiwa N, Toda Y. J Am Chem Soc 2002;124:1176–7.
[26] Imuta J, Toda Y, Matsugi T, Kaneko H, Matsuo S, Kojoh S, et al. Chem Lett 2003;32:656–7.
[27] Minoura Y, Ueda M, Mizunuma S, Oba M. J Appl Polym Sci 1969;13:1625–40.
[28] Kaneyoshi H, Matyjaszewski K. J Appl Polym Sci 2007;105:3–13.
[29] Matyjaszewski K, Xia J. Chem Rev 2001;101:2921–90.
[30] Kamigaito M, Ando T, Sawamoto M. Chem Rev 2001;101:3689–745.
[31] Lutz J-F, Matyjaszewski K. J Polym Sci Part A Polym Chem 2005;43:897–910.
[32] Naffakh M, Martín Z, Fanegas N, Marco C, Gómez MA, Jiménez I. J Polym Sci Part B Polym Phys 2007;45:2309–21.
[33] Wu J, Wu T, Chen W, Tsai S, Kuo W. J Polym Sci Part B Polym Phys 2005;43:3242–54.
[34] Zhang Y, Xin Z. J Appl Polym Sci 2006;100:4868–74.
[35] Habsuda J, Simon GP, Cheng YB, Hewitt DG, Diggins DR, Toh H, et al. Polymer 2002;43:4627–38.